Characterization of the Intrinsic and TSC2-GAP Regulated GTPase Activity of Rheb by Real-Time NMR

Christopher B. Marshall, Jason Ho, Claudia Buerger, Michael J. Plevin, Guang-Yao Li, Zhihong Li, Mitsuhiko Ikura and Vuk Stambolic (27 January 2009) *Science Signaling* **2** (55), ra3. [DOI: 10.1126/scisignal.2000029]

GTP HYDROLYSIS

Characterization of the Intrinsic and TSC2-GAP–Regulated GTPase Activity of Rheb by Real-Time NMR

Christopher B. Marshall,[1,2] Jason Ho,[1] Claudia Buerger,[1,2] Michael J. Plevin,[1,2] Guang-Yao Li,[1,2] Zhihong Li,[1,2] Mitsuhiko Ikura,[1,2]* Vuk Stambolic[1,2]*

(Published 27 January 2009; Volume 2 Issue 55 ra3)

Tuberous sclerosis complex 2 (TSC2), whose gene is frequently mutated in tuberous sclerosis, increases the guanosine triphosphatase (GTPase) activity of the small heterotrimeric GTP-binding protein (G protein) Rheb, thus resulting in the decreased activity of the mammalian target of rapamycin (mTOR), the master regulator of cell growth. Here, we describe the development of a nuclear magnetic resonance (NMR)–based, quantitative, real-time assay to explore the molecular mechanism of the intrinsic and TSC2-catalyzed GTPase activity of Rheb. We confirmed that TSC2 accelerated GTP hydrolysis by Rheb 50-fold through an "asparagine-thumb" mechanism to substitute for the nonfunctional "catalytic" glutamine of Rheb and we determined that catalysis was enthalpy driven. Most, but not all, of the disease-associated GTPase-activating protein (GAP) domain mutants of TSC2 that we examined affected its enzymatic activity. This method can now be applied to study the function and regulation of other GTPases.

INTRODUCTION

Rheb is a conserved, ubiquitously expressed, small guanosine triphosphatase (GTPase) that belongs to the Ras superfamily and has homologs in yeast, fungi, slime mold, fruit fly, zebra fish, and mammals (*1*–*3*). Genetic and biochemical studies have firmly established Rheb as a molecular switch that acts immediately downstream of a protein complex consisting of the products of the tumor suppressor genes *tuberous sclerosis complex 1* (*TSC1*) and *TSC2* (*4*–*8*). Mutations in these genes are associated with tuberous sclerosis, a disorder characterized by benign tumors (hamartomas) that affect the brain, kidneys, skin, heart, and lungs (*9*, *10*). In the guanosine triphosphate (GTP)–bound state, Rheb assumes an "on" conformation and, through a largely unexplored molecular mechanism, potently activates the protein kinase mammalian target of rapamycin (mTOR), the master regulator of global cellular protein synthesis and growth (*11*). mTOR influences the extent of cellular protein translation by phosphorylation and inhibition of 4E-BP1, a negative regulator of eukaryotic translation initiation factor 4E (eIF4E) (*12*, *13*). Another mTOR target, p70S6 kinase (p70S6K), broadly influences translation through the phosphorylation and activation of eIF4B and inhibition of eIF2 kinase (*14*) (fig. S1).

TSC2 is a GTPase-activating protein (GAP) and mediates this effect by interacting with its target proteins through its C-terminal GAP domain, which is homologous to that of Rap1GAP (*7*–*10*). Upon interacting with TSC2, GTP hydrolysis by Rheb is accelerated, which results in a conformational transition to the guanosine diphosphate (GDP)–bound "off" state of Rheb (*15*) and decreased mTOR activity. TSC2 (also known as tuberin) heterodimerizes with TSC1 (also known as hamartin) (*16*) to form a complex that integrates a number of homeostatic signals within the cell, including growth factors, nutrients, oxygen, and cellular energy status (*11*, *17*–*21*) (fig. S1). In response to cytokines and growth factors, the stability of the complex is disrupted through the phosphorylation of TSC2 by Akt (*18*, *19*, *22*), extracellular signal–regulated kinase (ERK) (*23*), or ribosomal S6 kinase (RSK) (*24*), as well as through the phosphorylation of TSC1 by cyclin-dependent kinase 1 (CDK1) (*25*) or inhibitor of nuclear factor κB (IκB) kinase β (IKKβ) (*26*). On the other hand, the TSC1-TSC2 complex is stabilized when TSC2 is phosphorylated by adenosine monophosphate (AMP)–activated protein kinase (AMPK) or glycogen synthase kinase 3 (GSK-3) in response to depletion of cellular energy (*21*, *27*) or through its interaction with the protein regulated in development and DNA damage responses (REDD1) in response to hypoxia (*28*).

Rheb is most closely related to the small GTPases H-Ras and Rap2, but differences in some key amino acid residues suggest that Rheb has a unique molecular mechanism of action, in particular the presence of an arginine residue (Arg^{15}) in the conserved position homologous to Gly^{12} of Ras. Mutations in Gly^{12} of Ras hinder its intrinsic GTPase activity and decrease its susceptibility to the activity of RasGAP (*29*–*33*). Consistent with this, Rheb exhibits a lower intrinsic rate of GTPase activity than that of Ras; however, the substitution $Arg^{15}\rightarrow Gly^{15}$ is not sufficient to increase the GTPase activity of Rheb (*2*, *34*, *35*). Further, although Rheb has a potentially catalytic glutamine residue (Gln^{64}), which is equivalent to Gln^{61} of Ras, the crystal structure of Rheb shows that Gln^{64} is buried in a hydrophobic pocket in an orientation that is incompatible with any involvement in catalysis (*15*) (Fig. 1A).

The molecular parameters underlying the low intrinsic GTPase activity of Rheb are not well understood, and the mechanism by which TSC2 catalyzes GTP hydrolysis is not clear. To study these mechanisms, we took advantage of advances in nuclear magnetic resonance (NMR) spectroscopy to develop a quantitative, dynamic, structure-based, real-time enzymatic assay to measure the GTPase activity of Rheb. With this method, we obtained a time-resolved record of intrinsic hydrolysis of GTP by Rheb and determined the reaction rates of wild-type (WT) and mutant Rheb proteins, directly probing the molecular mechanism of hydrolysis. Moreover, we examined the GAP activity of several TSC2 polypeptides,

[1]Division of Signaling Biology, Ontario Cancer Institute, University Health Network, Toronto, Ontario, Canada M5G 2M9. [2]Department of Medical Biophysics, University of Toronto, Toronto, Ontario, Canada M5G 2M9.
*To whom correspondence should be addressed. E-mail: vuks@uhnres.utoronto.ca (V.S.) and mikura@uhnresearch.ca (M.I.)

including disease-associated GAP domain mutants and engineered variants, providing a quantitative measure of their activity and dissecting the molecular mechanism of TSC2 GAP activity.

RESULTS

Structural distinction of nucleotide-dependent changes in Rheb by NMR

Based on the distinct structures of the crystalline forms of Rheb-GTP and Rheb-GDP (*15*), we anticipated that the NMR spectra of Rheb in solution would exhibit nucleotide-specific differences. We expressed the G-domain of Rheb (amino acid residues 1 to 169) in *Escherichia coli* and collected the ^{1}H-^{15}N heteronuclear single-quantum coherence (HSQC) NMR spectra of purified Rheb bound to either GDP or the nonhydrolyzable GTP analog guanosine 5′-[β,γ-imido]triphosphate (GMPPNP), respectively. The analysis of Rheb-GDP yielded a well-dispersed, high-quality HSQC spectrum (Fig. 1B), and backbone resonance assignments of about 140 peaks were obtained with standard triple-resonance NMR experiments (*36*) (fig. S2A). A stretch of residues within the switch II region (residues 66 to 73) could not be assigned because of peak broadening, which presumably arose from intermediate time-scale exchange between two or more conformational states. Analysis of Rheb-GMPPNP also produced a well-dispersed HSQC spectrum in which about half of the

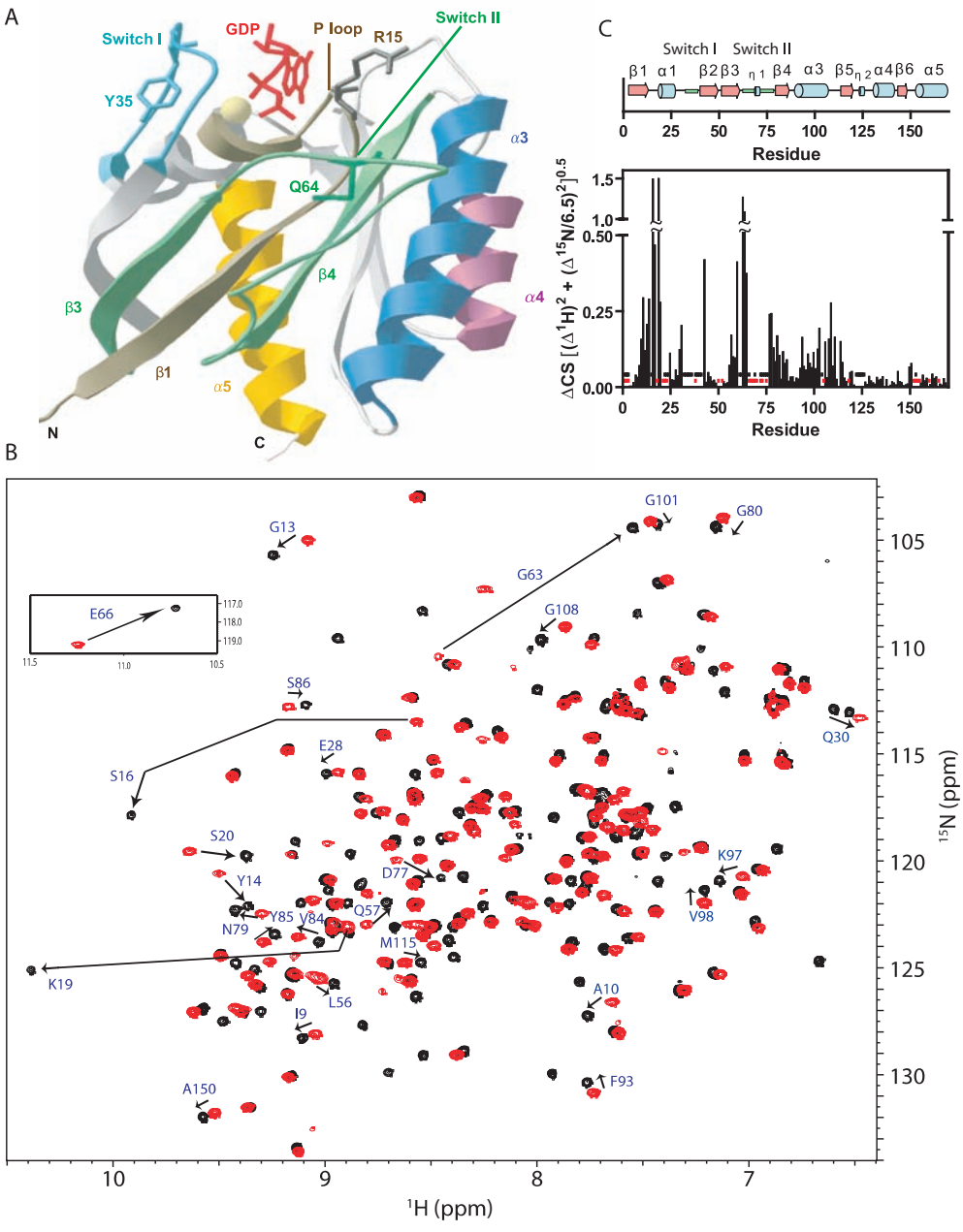

Fig. 1. Structure of Rheb and NMR spectral changes upon nucleotide cycling. (**A**) Crystal structure of Rheb-GDP [based on Protein Data Bank (PDB) 1XTQ (*15*)] with key structural elements and residues indicated. (**B**) ^{1}H-^{15}N HSQC spectra of Rheb in the GDP- and GMPPNP-bound states (black and red, respectively) with assignments of key residues and arrows to track changes in chemical shift. Full assignments are shown in fig. S2. Each spectrum represents an accumulation of 16 scans requiring a collection time of 80 min. (**C**) Secondary structure of Rheb and changes in chemical shift for Rheb-GDP versus Rheb-GMPPNP. Where residues were assigned in both spectra, normalized changes in chemical shift were calculated. Blue dots indicate residues that were not assigned in the GMPPNP-bound state and red dots indicate those residues that were not assigned for Rheb-GDP.

peaks exhibited chemical shift changes relative to those of Rheb-GDP, whereas a number of peaks were nearly superimposable on those of the Rheb-GDP spectrum (Fig. 1B). Broadening or complete loss of peaks were also observed. Residue-specific assignment was possible for 130 cross peaks in the ^{1}H-^{15}N HSQC spectrum of GMPPNP-bound Rheb (fig. S2B); however, residues corresponding to the switch I region (residues 31 to 42) were broadened and could not be assigned. This observation is consistent with the conformational heterogeneity of the switch regions seen in other GTPases (*37*).

Comparison of the HSQC spectra of GDP- and GMPPNP-bound Rheb identified elements associated with nucleotide-dependent structural changes. Specifically, amino acid residues in and around the nucleotide-binding pocket, including the P loop (residues 10 to 20) and switch II region (residues 60 to 65) displayed prominent changes in chemical shift (Fig. 1C). Chemical shift index (CSI) values (*38*) calculated for the assigned residues were in full agreement with the secondary structures of Rheb previously determined by x-ray crystallography (*15*) (fig. S3).

Development of a real-time, NMR-based assay for the analysis of the GTPase activity of Rheb

Because our HSQC spectra distinguish Rheb bound to the GTP analog from GDP-bound Rheb, we set out to monitor the change in the relative proportions of GTP-bound and GDP-bound Rheb over time as a way to measure the GTPase activity of Rheb. To load Rheb with unmodified GTP, it was incubated overnight with a 10-fold excess of GTP in the presence of 10 mM EDTA to promote nucleotide exchange and then saturated with Mg^{2+} and desalted by gel filtration (*39*) (fig. S4). EDTA was used to chelate Mg^{2+} and weaken the binding of nucleotide, whereas the subsequent addition of Mg^{2+} served to stabilize GTP binding to Rheb. The resulting Rheb preparations were typically >90% loaded with GTP (determined from peak ratios in ^{15}N HSQC spectra) and produced HSQC spectra similar to those of Rheb-GMPPNP.

To probe the intrinsic GTPase activity of Rheb in real time, multiple ^{15}N HSQC spectra of freshly prepared Rheb-GTP (400 μM, at 19°C) were collected successively during the hydrolysis reaction, initially every 5 min and then with decreasing frequency. The combination of high-field NMR (800 MHz) and a highly sensitive cryoprobe allowed us to collect reproducible spectra with high signal-to-noise ratios in less than 5 min (Fig. 2A). The first spectrum consisted of prominent cross peaks corresponding to Rheb-GTP with a subset of cross peaks from Rheb-GDP visible just above the noise level. As the hydrolysis of nucleotide proceeded, peaks corresponding to Rheb-GDP increased in intensity, while the peaks corresponding to Rheb-GTP decreased. Both sets of peaks exhibited similar intensities at ~12 hours, and by 44 hours the peaks corresponding to Rheb-GTP were reduced to the level of noise, indicating the complete turnover of GTP (Fig. 2A and fig. S5).

The intensities of each Rheb-GTP and Rheb-GDP cross peak were extracted from the spectra collected at each time point and the peak heights of well-resolved "reporter residues" were plotted against time (fig. S6). Peak heights corresponding to Rheb-GTP or Rheb-GDP were normalized to the initial spectrum (GTP-bound) and the final spectrum (GDP-bound), respectively, and well-resolved peaks were grouped based on their position within the structure of Rheb. Amino acid residues in each of four regions, (i) the β1 strand and the P loop, (ii) the switch I region, (iii) the β3 strand, the switch II region, and the β4 strand, and (iv) the α3 helix produced GTP-specific peaks that decreased in intensity with single-phase exponential decay kinetics and GDP-specific peaks that appeared with the same kinetics (Fig. 2B). These structural elements were near the nucleotide-binding site or the switch regions, consistent with the notion that the observed changes in NMR spectra reflect the GTPase reaction.

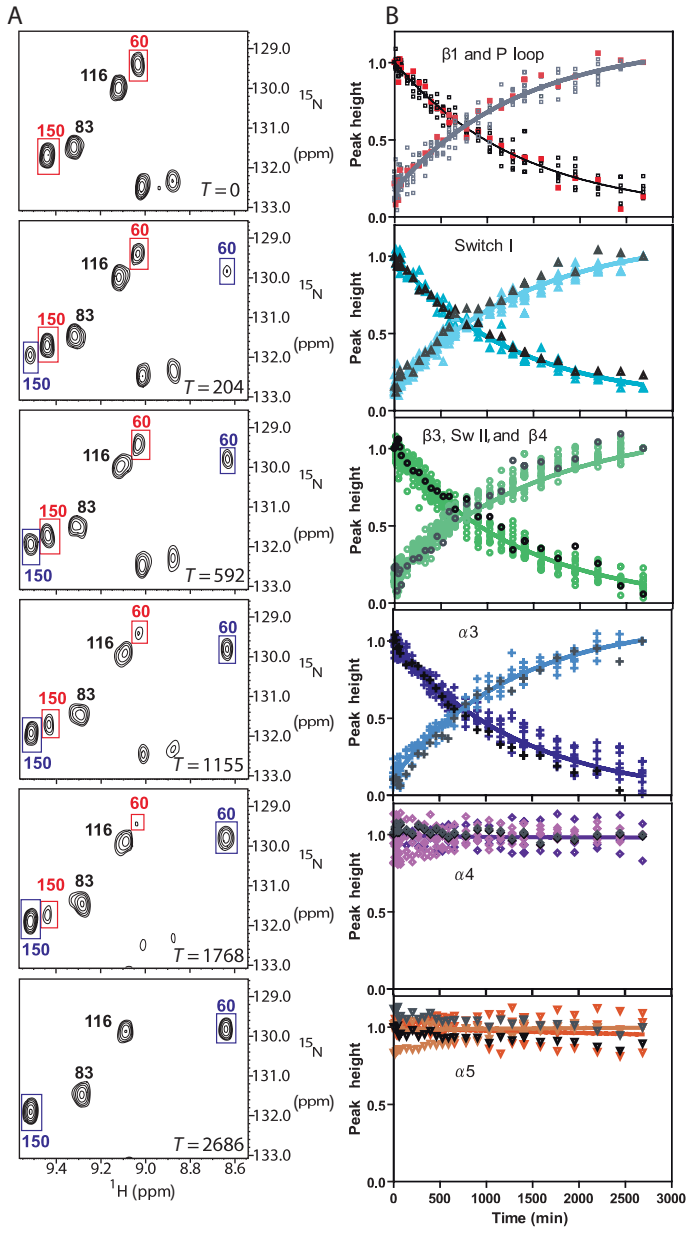

Fig. 2. Intrinsic GTPase activity of Rheb. (**A**) Snapshots of the HSQC spectra of GTP-loaded Rheb taken throughout the time course of GTP hydrolysis (time indicated in minutes). Peaks specific to Rheb-GTP are indicated in red, peaks corresponding to Rheb-GDP that appear as hydrolysis occurs are indicated in blue, and peaks that do not change with hydrolysis are labeled in black. (**B**) Peak heights for Rheb residues corresponding to GTP-bound (dark colors, normalized to T = 0) and GDP-bound (light colors, normalized to the end point of the hydrolysis reaction) states versus time. Residues are grouped according to structural elements and are colored to correspond to Fig. 1A. For each region, data points for a single residue are indicated in red or black (Y14, F31, Q57, K97, Q139, and A167). These data are derived from a representative GTPase experiment, with each time point representing two scans collected over 5 min.

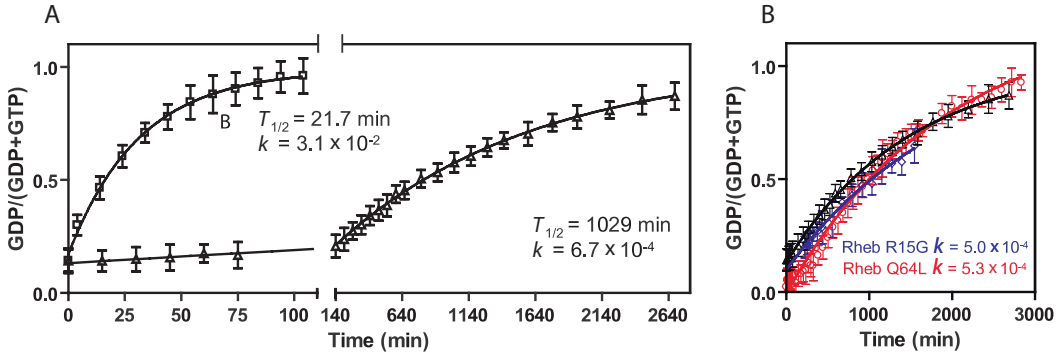

Fig. 3. Intrinsic GTPase activity and sensitivity to GAP activity of WT and mutant Rheb. (A) Hydrolysis of GTP by WT Rheb alone (triangles) or in the presence of $TSC2_{1525–1742}$ (squares) presented as a fraction of GDP for each time point based on peak heights $[I_{GDP}/(I_{GDP} + I_{GTP})]$ averaged for 22 residues. Error bars represent standard deviation of the fraction of GDP reported by the 22 residues. (B) Intrinsic GTPase activity of Rheb mutants R15G (blue diamonds) and Q64L (red circles) compared to that of WT Rheb (black triangles). Each curve is derived from a representative GTPase assay with multiple time points, each representing two scans.

In contrast, peaks corresponding to residues in the α4 and α5 helices displayed nearly identical positions and intensities (Fig. 2B). In total, dynamic changes in 22 amino acid residues of Rheb were used to derive a single curve reflective of the GTPase reaction (Fig. 3A). The fraction of Rheb bound to GDP was calculated on the basis of the intensity of each of the 22 peaks $[I_{GDP}/(I_{GDP} + I_{GTP})]$ at each time point and the averaged data fit an exponential decay curve with a rate of 6.7×10^{-4} min^{-1}, indicative of a GTP half-life of 1029 min (Fig. 3A).

Atypical of Ras subfamily members, Rheb contains an arginine residue (Arg^{15}) (Fig. 1A) at a position in which glycine is conserved (for example, Gly^{12} in Ras). Mutations of Gly^{12} (including Gly^{12}→Arg^{12}) reduce the intrinsic GTPase activity of Ras and severely impair the ability of RasGAPs to promote GTP hydrolysis by Ras (*30–33*, *40–43*). In mammalian cells, Rheb proteins with mutations in Arg^{15} exhibit similar GTP loading to WT Rheb and no difference in downstream signaling processes; however, the Rheb Arg^{15}→Gly^{15} mutant is partially resistant to the GAP activity of overexpressed TSC2 (*34*, *35*). To examine the importance of Arg^{15} for GTP hydrolysis, the GTPase activity of the Arg^{15}→Gly^{15} mutant Rheb was assessed by NMR. Consistent with previous studies, we found that this "Ras-like" mutation did not improve the catalytic activity of Rheb. Rather, this mutation decreased the intrinsic GTPase activity of Rheb by 25% (Fig. 3B), which has not been previously reported likely due to the limitations of thin-layer chromatography (TLC) as a detection method for measuring GTPase activity. Relative to the effect of mutation of the catalytic Gln^{61} of Ras, mutation of the homologous residue (Gln^{64}) in Rheb has less effect on GTP loading (*35*); however, the cell-based assay used could not completely distinguish between the effects of the mutation on the intrinsic GTPase activity of Rheb and those that affected the sensitivity of Rheb to GAP activity. Based on its orientation in the solved crystal structure of Rheb, it has been suggested that Gln^{64} may not participate in the hydrolysis of GTP (*15*). In our assay, a Gln^{64}→Leu^{64} mutant of Rheb had only slightly decreased catalytic activity compared to that of WT Rheb (Fig. 3B), further supporting the conclusion that, unlike in Ras, the conserved glutamine is not involved in hydrolysis. Taken together, these data provide a dynamic and quantitative measure of the GTPase activity of Rheb that is in full agreement with previous in vivo and in vitro studies, thus suggesting that our assay would also be useful for the study of the GAP activity of TSC2.

Characterization of the TSC2-GAP–catalyzed GTPase activity of Rheb

To investigate the activity and mechanism of action of the GAP domain of TSC2 (TSC2-GAP) with our NMR-based assay, various TSC2-GAP domain polypeptides were designed in light of its predicted secondary structure and homology to Rap1GAP. Among the constructs tested, we found that a polypeptide consisting of amino acid residues 1525 to 1742 of TSC2 ($TSC2_{1525–1742}$) exhibited the best expression and stability in *E. coli*. The N-terminal boundary of this construct was chosen so as to encompass all residues homologous to the catalytic domain of Rap1GAP. The C terminus of the construct was limited by the presence of a proteolytically labile site, which we identified by mass spectrometry as the Ala^{1742} to Arg^{1743} peptide linkage. Addition of $TSC2_{1525–1742}$ to Rheb-GTP at a 1:2 molar ratio increased Rheb's rate of GTP hydrolysis by 50-fold to 3.1×10^{-2} min^{-1} (Fig. 3A). Apart from accelerating the conversion of Rheb-GTP to Rheb-GDP, the GAP domain of $TSC2_{1525–1742}$ did not cause any discernable changes in the HSQC spectrum. Even when the GAP domain of $TSC2_{1525–1742}$ was added to GMPPNP-bound Rheb at a 1:1 molar ratio, no changes in the HSQC spectrum of Rheb were detected.

To assess the thermodynamic properties of the intrinsic and GAP-accelerated GTPase activities of Rheb, we examined the hydrolysis of GTP by Rheb alone and in the presence of the GAP domain of $TSC2_{1525–1742}$ at different temperatures. Using Arrhenius plots of reaction rate versus temperature (Fig. 4A), we calculated thermodynamic activation parameters for the hydrolysis of GTP, which allowed us to probe the unstable transition state that represents an energy barrier on the reaction pathway toward product formation. The minimum energy required to drive the reaction beyond this threshold is called the activation enthalpy ($\Delta H^{\ddagger}$). The reaction rate also depends on the activation entropy ($\Delta S^{\ddagger}$): the difference in entropy between the ground state and the transition state. Large negative values of $\Delta S^{\ddagger}$ indicate that disorder is reduced upon formation of the transition state, which is unfavorable for catalysis. Enzymes generally decrease $\Delta G^{\ddagger}$, the free energy of activation ($\Delta G^{\ddagger} = \Delta H^{\ddagger} - T\Delta S^{\ddagger}$), through stabilization of the transition state, which lowers the enthalpic component ($\Delta H^{\ddagger}$). Compared to the hydrolysis of GTP in water, Rheb reduces $\Delta H^{\ddagger}$ by 16.9 kJ/mol with little effect on $\Delta S^{\ddagger}$, thus reducing $\Delta G^{\ddagger}$ by 16.7 kJ/mol (Fig. 4B). Ras also promotes hydrolysis of GTP by reducing $\Delta H^{\ddagger}$, but to a greater extent than does Rheb (−21.5 kJ/mol) (*44*), resulting in a markedly faster reaction rate. The addition of substoichiometric quantities of the GAP domain of $TSC2_{1525–1742}$ (1:7 molar ratio) to Rheb further lowered $\Delta G^{\ddagger}$ by 6.8 kJ/mol at 25°C, consistent with the 50-fold increase in reaction rate. A substantial reduction in activation enthalpy by TSC2-GAP ($\Delta\Delta H^{\ddagger} = -46.3$ kJ/mol) was largely offset by an unfavorable decrease in activation entropy ($-T\Delta\Delta S^{\ddagger} = 39.5$ kJ/mol at 25°C), resulting in the modest overall reduction in free energy of activation. Taken together, the observed decreases in the enthalpic barriers for GTP hydrolysis by Rheb and Rheb–TSC2-GAP complex are consistent with a conventional enzymatic mechanism involving stabilization of the transition state.

Probing the catalytic mechanism of action of TSC2-GAP

Unlike the "arginine finger" mechanism used by the Ras and Rho GAPs to increase the GTPase activities of their target G proteins (*30*, *45*), the TSC2-GAP homolog, Rap1GAP, uses an asparagine residue (Asn^{290}) to promote nucleotide hydrolysis in the asparagine-thumb mechanism (*46*). The analogous residue in TSC2 (Asn^{1643}) is mutated to Lys, Ile, or His in patients with tuberous sclerosis (*47*–*50*), leading to deregulation of downstream signaling through Rheb (*7*, *35*). To assess the role of Asn^{1643} in the GAP activity of TSC2, we used our NMR-based assay to analyze TSC2 proteins mutated at this position. Mutation of Asn^{1643}→Ala^{1643} in $TSC2_{1525–1742}$ completely abolished its activity as a GAP (Fig. 5C), revealing that this residue is essential to the catalytic mechanism of TSC2. To investigate the role of the functional groups of the side chain of Asn^{1643} in catalysis, this residue was mutated to Asp. Complete loss of activity in the Asn^{1643}→Asp^{1643} mutant of $TSC2_{1525–1742}$ (Fig. 5C) showed that the amide group of the side chain was essential for catalysis. Moreover, the conservative mutation Asn^{1643}→Gln^{1643}, which preserves the functional group but extends the side chain, completely eliminated activity (Fig. 5C), highlighting a strict requirement for precise positioning of the catalytic carboxamide. Finally, to determine whether TSC2 and Rheb could coordinate a RasGAP-like arginine finger mechanism, an arginine residue was incorporated in place of Asn^{1643} of TSC2, which resulted in complete loss of its functions as a GAP (Fig. 5C).

To further dissect the catalytic mechanism, TSC2-GAP activity toward various Rheb mutants was assessed. The GTPase activity of the Arg^{15}→Gly^{15} mutant of Rheb was stimulated only 3.5-fold by $TSC2_{1525–1742}$ compared to the 50-fold enhancement of the GTPase activity of WT Rheb by $TSC2_{1525–1742}$ (Fig. 5F), consistent with a previous finding that this mutant is partially resistant to the GAP activity of TSC2 (*35*). Considering that RasGAP promotes GTP hydrolysis by Ras through an arginine finger mechanism (Fig. 6B), we examined whether a more "Ras-like" Arg^{15}→Gly^{15} mutant of Rheb could be affected by a "RasGAP-like" mutant of TSC2 by measuring the GTPase activity of the Arg^{15}→Gly^{15} Rheb mutant in the presence of the arginine finger $TSC2_{1525–1742}$ GAP mutant, $TSC2_{1525–1742}$ Asn^{1643}→Arg^{1643}, and found that the rate of GTP hydrolysis [$k = (6.4 \pm 0.5) \times 10^{-4}$ min^{-1}] was similar to that of the Arg^{15}→Gly^{15} mutant of Rheb alone. Whereas we had determined that the Gln^{64}→Leu^{64} mutation did not affect the intrinsic rate of hydrolysis of GTP by Rheb (Fig. 3B), we next investigated whether Gln^{64} was involved in the GAP-catalyzed hydrolysis of GTP. Indeed, Rheb Gln^{64}→Leu^{64} was substantially less susceptible to the GAP activity of $TSC2_{1525–1742}$, exhibiting a reaction rate 60% lower than that of WT Rheb in the presence of TSC2-GAP (Fig. 5F), which suggests that Gln^{64} may play some role in the mechanism by which the GAP domain of TSC2 increases the rate of GTP hydrolysis by Rheb.

Analysis of tuberous sclerosis–associated GAP domain mutations of TSC2

Certain mutations found in *TSC2* of patients with tuberous sclerosis map to the GAP domain of TSC2 (Fig. 5A) (*48*). Although mutations of Asn^{1643} directly affect the GAP activity of TSC2 (*7*, *35*), there has been no systematic characterization of the activities of other TSC2-GAP mutants. We applied our assay to examine how six disease-associated mutations affected the ability of TSC2 to act as a GAP. We chose to examine the effects of one mutation of the catalytic Asn (Asn^{1643}→Ile^{1643}) (*50*, *51*), two mutations found within a predicted helix that contains the catalytic residue, His^{1640}→Tyr^{1640} (*52*) and Lys^{1638}→Asn^{1638} (*51*), as well as three disease-associated mutations that are predicted to map to surface-exposed regions of the GAP domain proximal to the catalytic Asn^{1643}, Glu^{1558}→Lys^{1558} (*49*, *53*), Leu^{1594}→Met^{1594} (*48*), and Asp^{1690}→Tyr^{1690} (*54*) (Fig. 5B). The quality of each TSC2-GAP mutant protein preparation was assessed from their gel-filtration chromatograms and circular dichroism (CD) spectra (fig. S7). Consistent with the loss of activity associated with four other mutations of the catalytic Asn (Fig. 5C), the $TSC2_{1525–1742}$ Asn^{1643}→Ile^{1643} mutant was inactive (Fig. 5D). Likewise, disease-associated mutations of His^{1640} and Lys^{1638}, proximal to Asn^{1643}, as well as the more distal residue Glu^{1558} each eliminated the GAP activity of TSC2 (Fig. 5D). The conservative substitution Leu^{1594}→Met^{1594} resulted in an about 80% reduction in the GAP activity of TSC2 compared to that of WT TSC2 (Fig. 5D). Conversely, the Asp^{1690}→Tyr^{1690} mutation did not impair the GAP activity of TSC2, indicating that its effect on the pathology of tuberous sclerosis likely does not involve direct modulation

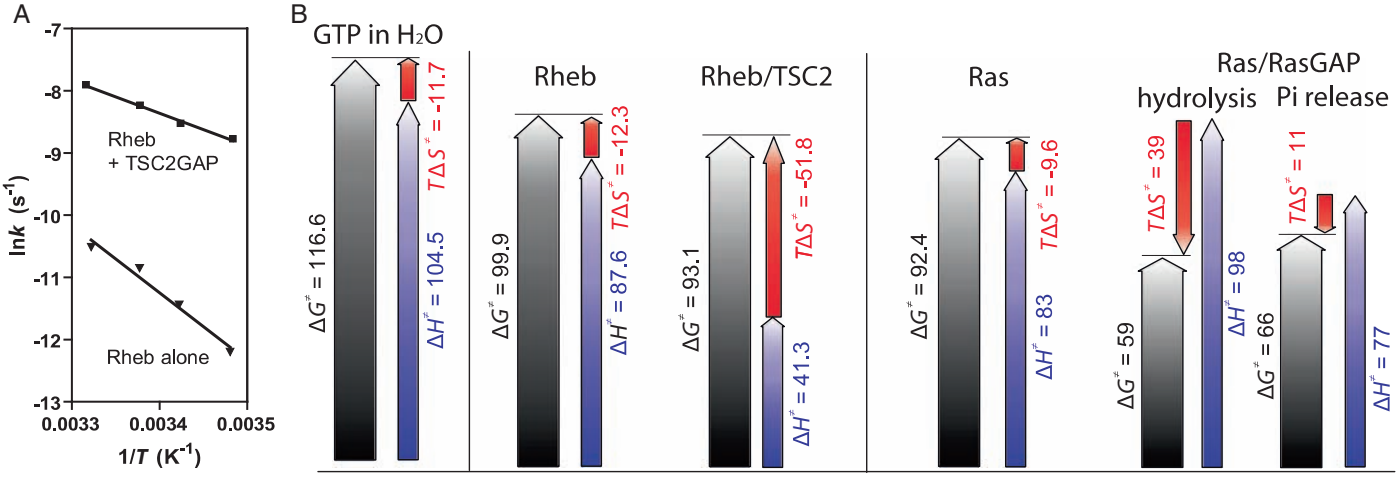

Fig. 4. Thermodynamic activation parameters for GTP hydrolysis by Rheb and the GAP domain of TSC2. (**A**) Arrhenius plots for GTP hydrolysis by Rheb alone (triangles) and in the presence of $TSC2_{1525–1742}$ (squares). Each data point represents a rate calculated from a representative GTPase assay consisting of 40 and 20 time points for Rheb alone and Rheb with TSC2, respectively. (**B**) Summary of thermodynamic activation parameters [free energy of activation ($\Delta G^{\ddagger}$), activation enthalpy ($\Delta H^{\ddagger}$), and activation entropy ($T\Delta S^{\ddagger}$) in kilojoules per mole] calculated for GTP hydrolysis by Rheb and Rheb–TSC2-GAP in this study, and, by way of comparison, for GTP alone, Ras, and Ras-RasGAP from Kötting *et al.* (*64*).

of GAP activity. It should be noted that all of the described TSC2 mutants produced similar CD spectra, except for Glu^{1558}→Lys^{1558}, which exhibited a CD spectrum that was slightly different from that of WT TSC2 (fig S7B). The spectrum of the Glu^{1558}→Lys^{1558} mutant was likely of poor quality because it was collected at a substantially lower concentration of protein than was the case for the other TSC2 mutants, due to its limited solubility and recovery when expressed in *E. coli*. Judged by this spectrum and its reduced solubility, we cannot rule out the possibility that the lack of GAP activity of this mutant could be due to partial misfolding of the protein.

Mapping the TSC2-GAP–binding site of Rheb

The GAP activities of the assayed disease-associated mutant TSC2 proteins highlighted some of the residues required for catalysis of GTP hydrolysis, binding to Rheb, or both. To map the Rheb-binding site on the TSC2-GAP domain in more detail, we engineered several mutations of TSC2 that have not been reported in patients with tuberous sclerosis. Phe^{1666} is a conserved residue that is predicted to be spatially adjacent to the asparagine thumb and is homologous to a Rap1GAP residue implicated in binding to Rap1 (*55*). The Phe^{1666}→Ala^{1666} mutation reduced the GAP activity of the mutant protein by 95% compared to that of WT TSC2 (Fig. 5E). Asp^{1598} and Glu^{1602}, together with the disease-associated site Leu^{1594}, reside within a predicted loop homologous to a region of Rap1GAP that is involved in extensive contacts with Rap1. Surprisingly, the Asp^{1598}→Ala^{1598} and Glu^{1602}→Ala^{1602} mutants of TSC2 exhibited full GAP activity. Taken together, our systematic analysis of TSC2-GAP mutants revealed certain similarities between TSC2 and Rap1GAP within

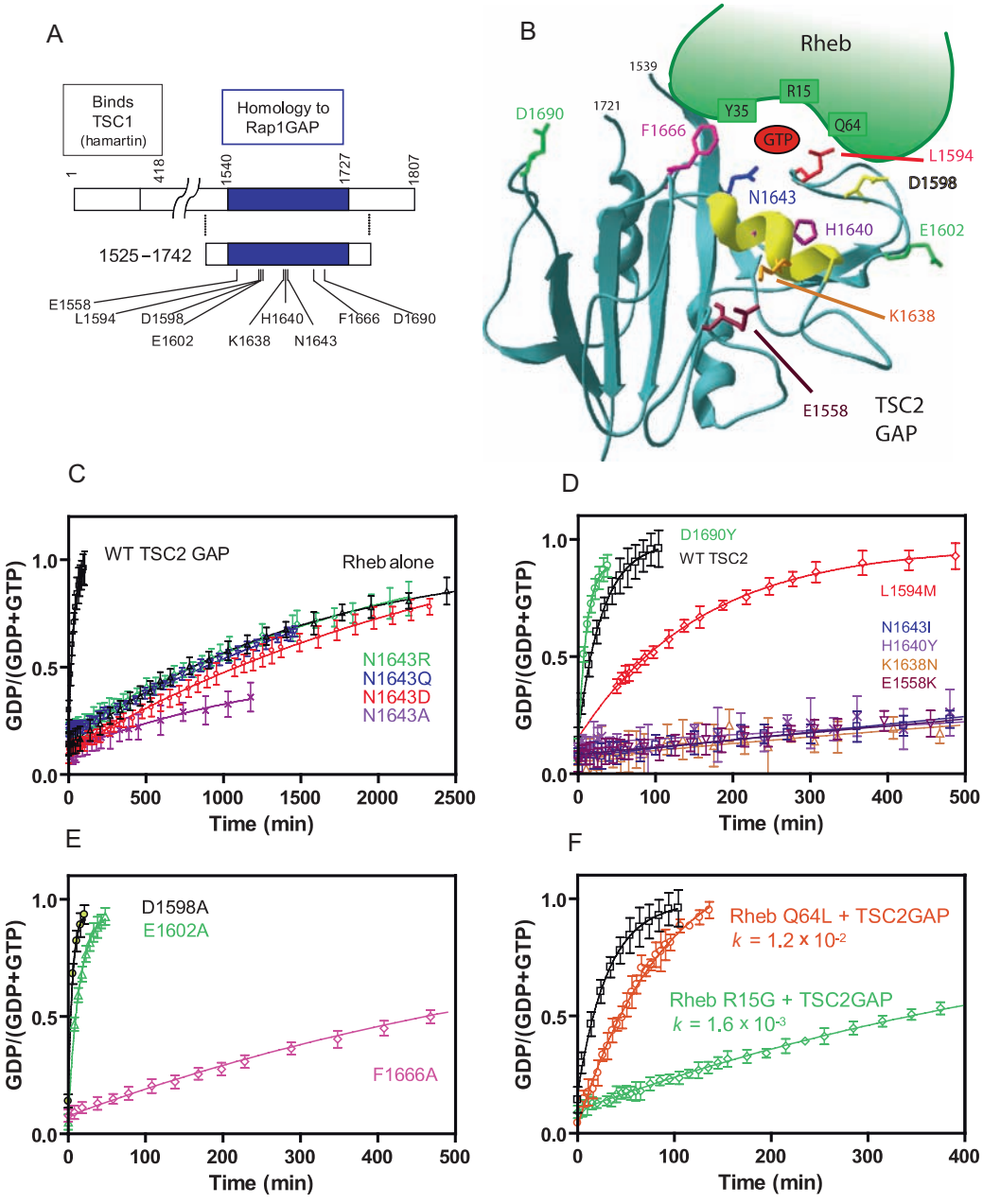

Fig. 5. Mutational analysis of the GAP activity of TSC2. (**A**) Domain map of TSC2 and the GAP domain construct indicating the positions of mutations investigated in this study. (**B**) Model of the GAP domain of TSC2 (residues 1539 to 1721) based on its homology to Rap1GAP (PDB 1SRQ) showing the position of the putative asparagine thumb, Asn^{1643}. The predicted locations of disease-associated and engineered mutations analyzed in this study are shown and the predicted helix that supports the asparagine thumb is highlighted in yellow. (**C**) GAP activity of Asn^{1643} mutants of $TSC2_{1525–1742}$ (N1643A, purple X; N1643D, red circles; N1643Q, blue inverted triangles; N1643R, green diamonds) versus WT $TSC2_{1525–1742}$ (black squares) and the intrinsic GTPase activity of Rheb alone (black triangles). (**D**) Effects of disease-associated mutations on the GAP activity of $TSC2_{1525–1742}$ (N1643I, blue squares; H1640Y, purple X; K1638N, orange diamonds; E1558K, dark red inverted triangles; L1594M, red diamonds; D1690Y, green circles; and WT $TSC2_{1525–1742}$, black squares). (**E**) Effects of engineered mutations on the GAP activity of $TSC2_{1525–1742}$ (D1598A, black circles; E1602A, green triangle; F1666A, pink diamonds). (**F**) GAP-catalyzed GTP hydrolysis by Rheb R15G (green diamonds) and Q64L (orange circles) relative to that of WT Rheb (black squares). Each curve in (C) to (F) presents the result of a representative GTPase assay in which each time point is an average of two scans and the error bars indicate the standard deviation of the fraction of GDP reported by 22 residues.

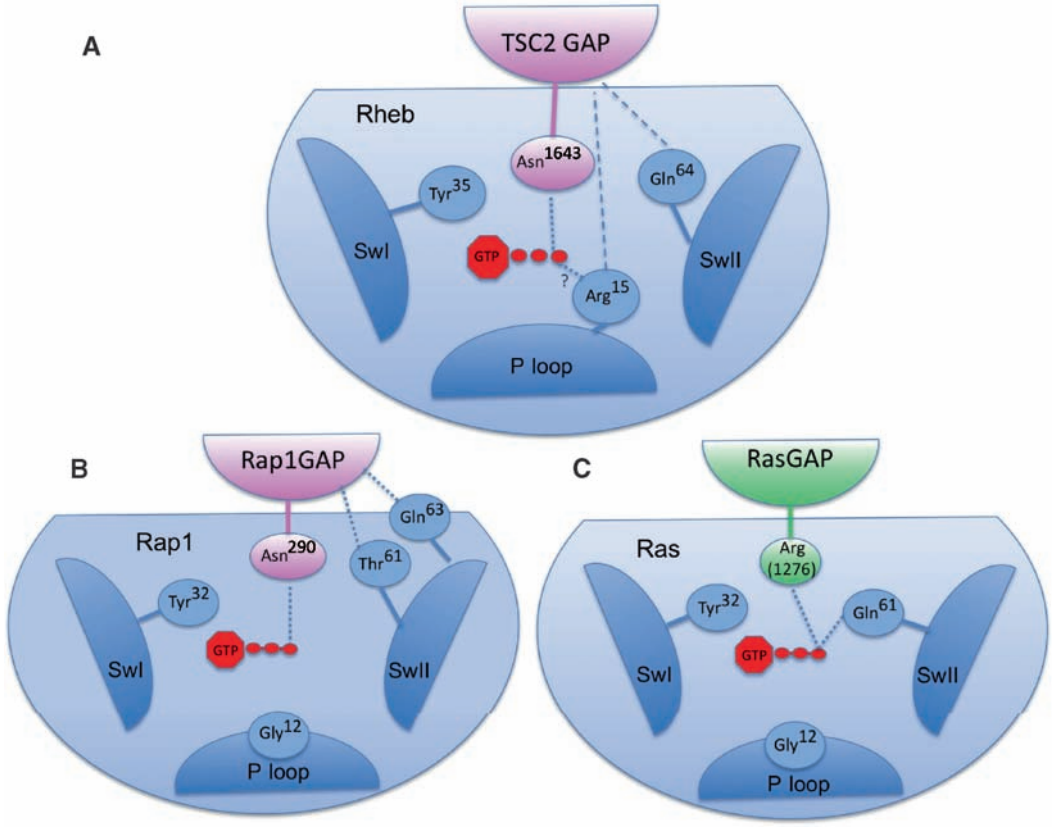

Fig. 6. Mechanisms of GAP activity. (**A**) TSC2 provides an asparagine thumb that substitutes for the Gln^{64} residue of Rheb, which is not catalytic but may form a protein-protein interaction with the GAP domain. Arg^{15}, which is not involved in the intrinsic mechanism of GTP hydrolysis, plays a role in the GAP-catalyzed reaction, either by promoting catalysis or by binding to the GAP. (**B**) Rap1 lacks the catalytic Gln^{61}, which is replaced by an asparagine thumb provided by Rap1GAP. SwI, switch I; SwII switch II. (**C**) RasGAP provides an arginine finger, which is directly involved in catalysis and stabilizes the catalytic Gln^{61} to promote activity.

the catalytic core, but key differences within the adjacent, partially conserved regions.

DISCUSSION

Based on the unique property of small GTPases that they tightly associate with both the substrate and the product of their enzymatic activity, thus assuming two distinct conformations, we have developed an NMR-based, real-time assay to analyze the intrinsic GTPase activity of Rheb and the GAP activity of TSC2. The present study is the first example of the use of two-dimensional heteronuclear NMR spectroscopy to provide a real-time comprehensive assay of the reaction kinetics of nucleotide hydrolysis by a heterotrimeric GTP-binding protein (G protein). This method relies on dynamic monitoring of changes in the chemical shifts of each amino acid residue, which are dependent on nucleotide-induced changes in the chemical environment and the structure of the protein. Among existing GTPase assays, those that use TLC or high-performance liquid chromatography (HPLC) to separate reaction products after the incubation of [β-^{32}P]GTP-loaded G protein are not consistent with determination of reaction kinetics or detection of subtle differences in GTPase activity. Although fluorescently tagged nucleotides have enabled real-time measurements of GTP hydrolysis for certain GTPases, not all G proteins are compatible with these modified nucleotides (*56*), and it cannot be predicted a priori whether a fluorescent label might interfere with the interactions between a GTPase and its regulators. The method presented here also eliminates many of the shortcomings of traditional approaches in that only well-folded protein contributes to the numeric output. Further, kinetic information is gathered for individual residues and can be directly correlated with the specific structural elements within the examined protein. Finally, our NMR-based method does not require chemical modifications of either the GTPase or the substrate, thus eliminating the biases introduced by their alterations.

Mechanistic aspects of intrinsic and TSC2-GAP–catalyzed hydrolysis of GTP by Rheb

Our work provides a quantitative measure of the rate of GTP hydrolysis by Rheb (with a half-life of ~17 hours at 19°C), which is 12- to 55-fold lower than the rates measured for various Ras isoforms (*44*, *57*–*59*). Consistently, previous end point measurements and metabolic labeling experiments have suggested that the intrinsic rate of GTP hydrolysis by Rheb is lower than that of Ras (*2*, *7*, *35*, *60*, *61*), and that Rheb isolated from cells is predominantly in the activated, GTP-bound state (*8*, *34*, *35*).

The high fidelity of our real-time, NMR-based assay allowed us to explore the activity of a minimal GAP domain of TSC2, which was previ-

ously thought to be inactive (*35*, *46*). We found that relatively high concentrations of the GAP domain of TSC2 were required to stimulate the GTPase reaction of Rheb (200 to 400 μM [^{15}N]Rheb was used to achieve high signal-to-noise ratios in the assay and the GAP domain of TSC2 added was half of that of [^{15}N]Rheb). Under these conditions, the measured half-life of GTP was ~22 min, similar to that determined by the HPLC-based assay reported by Scrima *et al*. (*55*). In contrast, when the GAP domain of TSC2 was used at a 1:50 molar ratio relative to Rheb, there was no enhancement of the GTP hydrolysis rate by Rheb [$k = (5.2 \pm 0.6) \times 10^{-4}$ min^{-1}]. The methodology developed here lays the groundwork for the characterization of full-length TSC2 and the TSC1-TSC2 heterodimer, which may determine whether other domains in this molecular complex contribute to its affinity for Rheb or to catalysis of the GTPase activity of Rheb.

GAP domains are diverse both in their structures and in the mechanisms by which they act on their cognate G proteins (*62*). RasGAPs stabilize the Gln^{61} residue of Ras in a catalytically competent position and insert an arginine finger that interacts with the β and γ phosphates of GTP and stabilizes the transition state of the hydrolysis reaction (*30*). Although they are structurally divergent, RhoGAPs also function by a remarkably similar mechanism (*45*). The GAP domain of TSC2 is distinct from those of other GAPs, but is homologous to the catalytic domain of Rap1GAP, which uses a catalytic, asparagine thumb that appears to substitute for the catalytic glutamine that is absent in Rap1 (*46*, *55*, *63*). Our results strongly support the asparagine-thumb mechanism for the action of the GAP domain of TSC2, because mutation of Asn^{1643} to Ala, Asp, Gln, Arg, or Ile completely eliminated its GAP activity (Fig. 5, C and D). Inactivation of the GAP activity of TSC2 by the Asn^{1643}→Asp^{1643} mutation (Fig. 5C) highlighted the importance of the amide group. The complete loss of GAP activity of TSC2 after the Asn^{1643}→Gln^{1643} mutation (Fig. 5C) showed the strict requirement for the appropriate positioning of the carboxamide of the asparagine thumb, which may interact with the nucleophilic water molecule (*55*). Not surprisingly, the Asn^{1643}→Arg^{1643} mutant TSC2 protein failed to act as a GAP with either WT Rheb or the Ras-like Arg^{15}→Gly^{15} mutant of Rheb, indicating that the GAP domain of TSC2 is incompatible with an arginine finger–like catalytic mechanism.

Given the importance of the Asn^{1643} residue of TSC2 for catalysis of GTP hydrolysis by Rheb, we investigated whether this residue replaced the Gln^{64} of Rheb during GTP hydrolysis. The Gln^{64}→Leu^{64} mutant of Rheb was less sensitive than WT Rheb to the GAP activity of TSC2; however, the rate of its hydrolysis of GTP was still stimulated >20-fold by the GAP domain of TSC2 (Fig. 5F), implying that Gln^{64} of Rheb, unlike Gln^{61} of Ras, did not directly participate in GTP hydrolysis (Fig. 6). Rather, the modest reduction by this substitution of the sensitivity of the mutant protein to the GAP activity of TSC2 suggested that Gln^{64} of Rheb may contribute to proper association or complex formation with the GAP domain. Similarly, Thr^{61}, which is in the equivalent position in Rap1 to Gln^{64} of Rheb, is not catalytic, but its mutation disrupts the interaction between Rap1 and Rap1GAP (*55*, *63*).

Mutation of Gly^{12} of Ras not only impairs its intrinsic GTPase activity, but also eliminates the ability of the RasGAPs to promote GTP hydrolysis by Ras (*30–33*, *40–43*). Rheb contains an Arg in the equivalent position and our results showed that the Arg^{15}→Gly^{15} mutation had little effect on the intrinsic rate of GTP hydrolysis, but reduced the sensitivity of mutant Rheb to the GAP activity of TSC2$_{1525–1742}$ by 95% compared to that of WT Rheb. This is consistent with the possibility that Arg^{15} of Rheb is critical for the optimal interaction between Rheb and TSC2. Alternatively, the positively charged side chain of Arg^{15} may be aligned by the GAP domain of TSC2 such that it contributes to the catalytic mechanism.

Thermodynamic considerations of GTP hydrolysis by Rheb and TSC2-GAP

We studied the temperature dependence of rates of GTP hydrolysis and compared the thermodynamic activation parameters for the hydrolysis of GTP by Rheb to those previously reported for Ras. Like Ras, Rheb catalyzes GTP hydrolysis primarily by lowering the activation enthalpy, although Rheb is less potent than Ras ($\Delta\Delta H^{\ddagger} = -16.9$ kJ/mol for Rheb compared to $\Delta\Delta H^{\ddagger} = -21.7$ kJ/mol for Ras), resulting in a higher free energy of activation (99.9 kJ/mol compared to 92.4 kJ/mol) and a slower reaction rate (Fig. 4, A and B). Addition of the GAP domain of TSC2 to Rheb substantially reduced the activation enthalpy (from 87.6 to 41.3 kJ/mol), which was offset in part by a large decrease in activation entropy (from −12.3 to −51.8 kJ/mol). This is in contrast to the RasGAP neurofibromin (NF1), which drives the hydrolysis of GTP by increasing the activation entropy (−9.6 to +39 kJ/mol for the cleavage reaction) (*64*). This increase in entropy is achieved by an unconventional mechanism in which displacement of ordered water molecules from the Ras-binding pocket upon insertion of the arginine finger of NF1 provides an entropic contribution of free energy that may be used toward bond cleavage.

In contrast, our results indicate that TSC2 uses a more conventional enthalpy-driven enzymatic reaction mechanism, which typically involves stabilization of the transition state through electrostatic interactions (*65*). The thermodynamic differences between NF1 and TSC2 indicate distinct structural bases for the reactions. The asparagine thumb of TSC2 does not fill the nucleotide-binding pocket of Rheb and is unlikely to displace water molecules. Rather, formation of a structurally stabilized GAP domain-Rheb complex may be entropically unfavorable. The asparagine thumb likely contributes to the reduced activation enthalpy in a manner analogous to that of Gln^{61} of Ras; however, the large effect on $\Delta H^{\ddagger}$ suggests that auxiliary mechanisms may contribute to GTP hydrolysis. These results show that the entropic mechanism proposed for RasGAP by Kötting and co-workers (*64*) cannot be generalized for all GAPs. Further structural studies will be needed to fully elucidate the details of the catalytic activity of GAP domain of TSC2.

The effect of polymorphisms and disease-associated mutations of TSC2

Our analysis has shown that most disease-associated mutants of TSC2 affect its catalytic activity. Based on the shared asparagine thumb–based catalytic mechanism and sequence homology between Rap1GAP and TSC2, we analyzed the GAP activity of a series of tuberous sclerosis–associated mutations in TSC2 that were predicted to occur at surface residues (Fig. 5B). Consistent with our analysis of other mutations of the asparagine thumb (Fig. 5C), the disease mutation Asn^{1643}→Ile^{1643} (*50*, *51*) eliminated the activity of the GAP domain of the mutant TSC2, which strongly suggested that the inability to inactivate Rheb underlies the pathogenesis of this mutation, as is likely the case with the other disease-associated mutations at this position: Asn^{1643}→His^{1643} (*49*) and Asn^{1643}→Lys^{1643} (*48*).

The catalytic Asn of Rap1GAP is situated at the C terminus of an eight-residue helix (*46*), which is conserved in TSC2. We found that tuberous sclerosis–associated mutations in two invariant residues within this helix, His^{1640}→Tyr^{1640} (*52*) and Lys^{1638}→Asn^{1638} [Leiden Open Variation Database (LOVD)], eliminated GAP activity (Fig. 5D). The solved structures of Rap1GAP (*46*, *55*) suggest that these residues, which correspond to His^{287} and Lys^{285} in Rap1GAP, respectively, are important for proper positioning of the helix, and thus of the catalytic Asn of TSC2, for catalysis. The Lys^{285} residue of Rap1GAP forms an intramolecular salt bridge with the invariant Glu^{207}, and mutation of either of these residues profoundly impairs the activity of Rap1GAP (*46*, *55*, *66*). Likewise, a tuberous sclerosis–associated TSC2 mutant, Glu^{1558}→Lys^{1558}

(*49*, *53*), which is homologous to Glu^{207} of Rap1GAP, abolished its GAP activity (Fig. 5D), possibly by destabilizing the structure of the GAP domain.

The complete loss of activity associated with these mutations is likely due directly to disrupted catalytic function. To identify residues of the GAP domain of TSC2 involved in binding to Rheb, we analyzed disease-associated mutations and engineered mutations of residues predicted to be proximal to the catalytic residue in the three-dimensional structure of TSC2. Phe^{1666} of TSC2 is conserved and equivalent to Phe^{313} of Rap1GAP, which forms part of a hydrophobic binding site for Rap1 beside the asparagine thumb. The mutation Phe^{1666}→Ala^{1666} reduced the GAP activity of TSC2 by 95% compared to that of WT TSC2 (Fig. 5E), suggesting that a hydrophobic patch similar to that of Rap1GAP plays a role in the docking of Rheb with TSC2. On the other side of the asparagine thumb, a long loop in Rap1GAP is involved in extensive protein-protein contacts with Rap1 (*55*), and several disease-associated mutations have been found in the corresponding region of TSC2, including Leu^{1594}→Met^{1594} (*48*), Gly^{1595}→Arg^{1595} (LOVD), and Leu^{1597}→Pro^{1597} (*49*). Surprisingly, a conservative Leu^{1594}→Met^{1594} substitution at this position substantially reduced the GAP activity of TSC2 (Fig. 5D). Because fully active Rap1GAP contains a divergent Arg at the position homologous to the Leu^{1594} of TSC2, this implicates this region in determining the specificities of these GAPs toward their cognate GTPases. To examine the role of a conserved residue within this loop, we designed a mutation of a strictly conserved residue, Asp^{1598}, which is homologous to Asp^{244} of Rap1GAP, which appears to be important for binding to Rap1. Nevertheless, the Asp^{1598}→Ala^{1598} mutation had no effect on the GAP activity of TSC2, revealing further differences between Rap1 and TSC2 in this region. Likewise, mutation of TSC2 Glu^{1602} to Ala did not reduce its GAP activity. Finally, we found that the disease-associated TSC2 mutation of Asp^{1690}, a residue found variant in independent cohorts of patients with tuberous sclerosis (LOVD), to Tyr surprisingly had no effect on GAP activity. Participation of this residue in the pathology of tuberous sclerosis is likely mediated by another aspect of TSC2 function, such as its interaction with TSC1, its intracellular trafficking, its stability, or its susceptibility to regulatory posttranslational modifications such as phosphorylation.

Implications for the analysis of other GTPases

The real-time, NMR-based method described here can, in principle, be applied to any G protein, as well as to the analysis of the regulatory effect of their cognate GAPs and GEFs. In the case of Rheb, considering its relatively low intrinsic GTPase activity, the frequency and the duration of collection of each HSQC spectrum was not a factor in deriving the rate of GTP hydrolysis. However, for the analysis of more efficient GTPases, such as Ras and Rho, the temporal resolution of data collection can be substantially improved on by the recently developed band-selective optimized flip-angle short transient (SOFAST) NMR pulse sequence, which facilitates collection of two-dimensional heteronuclear multiple quantum coherence (HMQC) spectra with a temporal resolution of a few seconds (*67*). We used this methodology to perform a real-time, NMR-based assay of GAP activity in which each spectrum was collected in 30 s (fig. S8). The rate of this TSC2-GAP–catalyzed reaction is comparable to the intrinsic GTPase rate of Ras, and >70 data points were obtained to monitor the reaction. Capturing the extremely rapid RasGAP-catalyzed reactions would be challenging, but might be accomplished by titration of the concentration of the GAP protein to achieve a suitable reaction rate. Another challenge to studying highly active GTPases is in obtaining fully GTP-loaded protein preparations. This could be overcome through the use of photocaged GTP analogs, which remain stable in complex with the G protein until their activation by a pulse of light (*68*). Finally, although the current protocol requires substantial quantities of protein (500 μl of sample at a concentration of ≥200 μM, or >2 mg per assay), we have obtained reasonable results with as little as 30 μl of sample at a concentration of ≤200 μM (~100 μg total protein) with a recently developed 1.7-mm microcryoprobe (Bruker Biospin) (fig. S9). Despite these challenges, real-time NMR enables the acquisition of temporally resolved, structure-specific data with nonradioactive, unmodified, natural nucleotides, which should provide further mechanistic detail and a deeper understanding of the nucleotide catalysis reactions of many small GTPases.

MATERIALS AND METHODS

Sample preparation and resonance assignments

The G domain of Rheb (residues 1 to 169, with the C-terminal hypervariable region and the CAAX box truncated) was expressed as a glutathione-*S*-transferase (GST) fusion protein from PGEX2T in the *E. coli* strain BL21 DE3 Codon+ by induction with 0.2 mM isopropyl-β-D-thiogalactopyranoside at 15°C overnight and enriched by binding to a glutathione-Sepharose resin. Rheb was cleaved from GST on the resin with thrombin and further purified by gel-filtration chromatography (S-75). Recombinant Rheb expressed in *E. coli* was purified primarily in the GDP-bound form. GMPPNP-bound Rheb was prepared by adding an excess of this nonhydrolyzable GTP analog in the presence of EDTA to decrease the affinity of GDP and calf instestinal alkaline phosphatase to degrade GDP (*39*). [^{13}C-^{15}N]Rheb and deuterated [^{13}C-^{15}N]Rheb were produced in M9 media supplemented with [^{13}C]glucose and [^{15}N]ammonium chloride, and triple-resonance experiments were performed to assign backbone resonances (see Supplementary Methods). For GTPase assays, [^{15}N]Rheb was loaded with GTP by incubation with a 10-fold excess of GTP in the presence of EDTA. After replenishing Mg^{2+}, excess nucleotide and EDTA were removed with a desalting column and the HSQC spectra were collected as soon as possible.

NMR-based GTPase assay

^{1}H-^{15}N sensitivity–enhanced HSQC spectra (two scans) were collected on a Bruker Advance II 800-MHz spectrometer equipped with a 5-mm TCI CryoProbe. The concentration of Rheb was 0.2 to 0.5 mM, and acquisition of each spectrum required 5 min. NMR spectra were processed and analyzed with NMRpipe (*69*). Cross peaks were picked and assigned in the reference spectra to create Rheb-GTP (first spectrum) and Rheb-GDP (last spectrum); peak lists and peak heights were extracted for each spectrum. The fraction of Rheb in the GDP-bound form [$I_{GDP}/(I_{GDP} + I_{GTP})$] was calculated from the peak intensities (I) of 22 reporter residues, plotted against time, and fit to a one-phase exponential decay curve. A construct encoding residues 1525 to 1742 of TSC2 was cloned into pGEX2T, expressed in LB medium and purified as described for Rheb. A homology model of the GAP domain of TSC2 including residues 1539 to 1721 was constructed with SWISS-MODEL (*70*) with Rap1GAP (PDB 1SRQ) as a template. To assay GTP hydrolysis in the presence of the GAP domain, a reference spectrum of GTP-loaded Rheb was collected; a small volume of highly concentrated GAP in NMR buffer was added (in a 1:2 molar ratio) and a series of spectra were collected, initially at 5-min intervals. Mutants of Rheb and TSC2 were generated with Quikchange (Stratagene) and sequences were confirmed by DNA sequencing.

Thermodynamic activation parameters for GTPase activity of Rheb alone and with TSC2

To measure the thermodynamic activation parameters for GTP hydrolysis by Rheb alone and for the TSC2-GAP–catalyzed reaction, the

NMR-based GTPase assay was performed at four different temperatures (287, 292, 296, and 301.5 K). $TSC2_{1525–1742}$ was added to Rheb at a molar ratio of 1:7. Arrhenius plots were constructed by plotting $\ln(k)$ as a function of $1/T$ and were then used to calculate activation energy (E_a), activation entropy ($\Delta S^{\ddagger}$), activation enthalpy ($\Delta H^{\ddagger}$), and free energy of activation ($\Delta G^{\ddagger}$).

SUPPLEMENTARY MATERIALS

www.sciencesignaling.org/cgi/content/full/2/55/ra3/DC1
Methods
Fig. S1. Role of Rheb in mTOR signaling.
Fig. S2. Spectra of Rheb-GDP and Rheb-GMPPNP.
Fig. S3. Secondary structure and chemical shift index analysis.
Fig. S4. Preparation of Rheb-GTP for GTPase assay.
Fig. S5. Time course of GTP hydrolysis of Rheb-GTP.
Fig. S6. Analysis of Rheb-GTP and Rheb-GDP during GTP hydrolysis.
Fig. S7. Circular dichroism spectra of WT $TSC2_{1225–1742}$ and its variants.
Fig. S8. Further development of real-time NMR method to increase temporal resolution.
Fig. S9. Further development of real-time NMR method to decrease sample requirement.
References

REFERENCES AND NOTES

1. G. W. Reuther, C. J. Der, The Ras branch of small GTPases: Ras family members don't fall far from the tree. *Curr. Opin. Cell Biol.* **12**, 157–165 (2000).
2. K. Yamagata, L. K. Sanders, W. E. Kaufmann, W. Yee, C. A. Barnes, D. Nathans, P. F. Worley, *rheb*, a growth factor– and synaptic activity–regulated gene, encodes a novel Ras-related protein. *J. Biol. Chem.* **269**, 16333–16339 (1994).
3. A. P. Tabancay Jr., C. L. Gau, I. M. Machado, E. J. Uhlmann, D. H. Gutmann, L. Guo, F. Tamanoi, Identification of dominant negative mutants of Rheb GTPase and their use to implicate the involvement of human Rheb in the activation of p70S6K. *J. Biol. Chem.* **278**, 39921–39930 (2003).
4. H. Stocker, T. Radimerski, B. Schindelholz, F. Wittwer, P. Belawat, P. Daram, S. Breuer, G. Thomas, E. Hafen, Rheb is an essential regulator of S6K in controlling cell growth in *Drosophila*. *Nat. Cell Biol.* **5**, 559–565 (2003).
5. L. J. Saucedo, X. Gao, D. A. Chiarelli, L. Li, D. Pan, B. A. Edgar, Rheb promotes cell growth as a component of the insulin/TOR signalling network. *Nat. Cell Biol.* **5**, 566–571 (2003).
6. A. Garami, F. J. Zwartkruis, T. Nobukuni, M. Joaquin, M. Roccio, H. Stocker, S. C. Kozma, E. Hafen, J. L. Bos, G. Thomas, Insulin activation of Rheb, a mediator of mTOR/S6K/4E-BP signaling, is inhibited by TSC1 and 2. *Mol. Cell* **11**, 1457–1466 (2003).
7. Y. Zhang, X. Gao, L. J. Saucedo, B. Ru, B. A. Edgar, D. Pan, Rheb is a direct target of the tuberous sclerosis tumour suppressor proteins. *Nat. Cell Biol.* **5**, 578–581 (2003).
8. K. Inoki, Y. Li, T. Xu, K. L. Guan, Rheb GTPase is a direct target of TSC2 GAP activity and regulates mTOR signaling. *Genes Dev.* **17**, 1829–1834 (2003).
9. P. B. Crino, K. L. Nathanson, E. P. Henske, The tuberous sclerosis complex. *N. Engl. J. Med.* **355**, 1345–1356 (2006).
10. J. Huang, B. D. Manning, The TSC1-TSC2 complex: A molecular switchboard controlling cell growth. *Biochem. J.* **412**, 179–190 (2008).
11. D. J. Kwiatkowski, B. D. Manning, Tuberous sclerosis: A GAP at the crossroads of multiple signaling pathways. *Hum. Mol. Genet.* **14** (Spec No. 2), R251–R258 (2005).
12. L. Beretta, A. C. Gingras, Y. V. Svitkin, M. N. Hall, N. Sonenberg, Rapamycin blocks the phosphorylation of 4E-BP1 and inhibits cap-dependent initiation of translation. *EMBO J.* **15**, 658–664 (1996).
13. A. C. Gingras, B. Raught, N. Sonenberg, Regulation of translation initiation by FRAP/mTOR. *Genes Dev.* **15**, 807–826 (2001).
14. I. Ruvinsky, O. Meyuhas, Ribosomal protein S6 phosphorylation: From protein synthesis to cell size. *Trends Biochem. Sci.* **31**, 342–348 (2006).
15. Y. Yu, S. Li, X. Xu, Y. Li, K. Guan, E. Arnold, J. Ding, Structural basis for the unique biological function of small GTPase RHEB. *J. Biol. Chem.* **280**, 17093–17100 (2005).
16. M. van Slegtenhorst, M. Nellist, B. Nagelkerken, J. Cheadle, R. Snell, A. van den Ouweland, A. Reuser, J. Sampson, D. Halley, P. van der Sluijs, Interaction between hamartin and tuberin, the TSC1 and TSC2 gene products. *Hum. Mol. Genet.* **7**, 1053–1057 (1998).
17. M. P. DeYoung, P. Horak, A. Sofer, D. Sgroi, L. W. Ellisen, Hypoxia regulates TSC1/2-mTOR signaling and tumor suppression through REDD1-mediated 14-3-3 shuttling. *Genes Dev.* **22**, 239–251 (2008).
18. K. Inoki, Y. Li, T. Zhu, J. Wu, K. L. Guan, TSC2 is phosphorylated and inhibited by Akt and suppresses mTOR signalling. *Nat. Cell Biol.* **4**, 648–657 (2002).
19. B. D. Manning, A. R. Tee, M. N. Logsdon, J. Blenis, L. C. Cantley, Identification of the tuberous sclerosis complex–2 tumor suppressor gene product tuberin as a target of the phosphoinositide 3-kinase/Akt pathway. *Mol. Cell* **10**, 151–162 (2002).
20. J. Avruch, K. Hara, Y. Lin, M. Liu, X. Long, S. Ortiz-Vega, K. Yonezawa, Insulin and amino-acid regulation of mTOR signaling and kinase activity through the Rheb GTPase. *Oncogene* **25**, 6361–6372 (2006).
21. K. Inoki, T. Zhu, K. L. Guan, TSC2 mediates cellular energy response to control cell growth and survival. *Cell* **115**, 577–590 (2003).
22. H. C. Dan, M. Sun, L. Yang, R. I. Feldman, X. M. Sui, C. C. Ou, M. Nellist, R. S. Yeung, D. J. Halley, S. V. Nicosia, W. J. Pledger, J. Q. Cheng, Phosphatidylinositol 3-kinase/Akt pathway regulates tuberous sclerosis tumor suppressor complex by phosphorylation of tuberin. *J. Biol. Chem.* **277**, 35364–35370 (2002).
23. L. Ma, Z. Chen, H. Erdjument-Bromage, P. Tempst, P. P. Pandolfi, Phosphorylation and functional inactivation of TSC2 by Erk implications for tuberous sclerosis and cancer pathogenesis. *Cell* **121**, 179–193 (2005).
24. P. P. Roux, B. A. Ballif, R. Anjum, S. P. Gygi, J. Blenis, Tumor-promoting phorbol esters and activated Ras inactivate the tuberous sclerosis tumor suppressor complex via p90 ribosomal S6 kinase. *Proc. Natl. Acad. Sci. U.S.A.* **101**, 13489–13494 (2004).
25. A. Astrinidis, W. Senapedis, T. R. Coleman, E. P. Henske, Cell cycle–regulated phosphorylation of hamartin, the product of the tuberous sclerosis complex 1 gene, by cyclin-dependent kinase 1/cyclin B. *J. Biol. Chem.* **278**, 51372–51379 (2003).
26. D. F. Lee, H. P. Kuo, C. T. Chen, J. M. Hsu, C. K. Chou, Y. Wei, H. L. Sun, L. Y. Li, B. Ping, W. C. Huang, X. He, J. Y. Hung, C. C. Lai, Q. Ding, J. L. Su, J. Y. Yang, A. A. Sahin, G. N. Hortobagyi, F. J. Tsai, C. H. Tsai, M. C. Hung, IKKβ suppression of TSC1 links inflammation and tumor angiogenesis via the mTOR pathway. *Cell* **130**, 440–455 (2007).
27. K. Inoki, H. Ouyang, T. Zhu, C. Lindvall, Y. Wang, X. Zhang, Q. Yang, C. Bennett, Y. Harada, K. Stankunas, C. Y. Wang, X. He, O. A. MacDougald, M. You, B. O. Williams, K. L. Guan, TSC2 integrates Wnt and energy signals via a coordinated phosphorylation by AMPK and GSK3 to regulate cell growth. *Cell* **126**, 955–968 (2006).
28. J. Brugarolas, K. Lei, R. L. Hurley, B. D. Manning, J. H. Reiling, E. Hafen, L. A. Witters, L. W. Ellisen, W. G. Kaelin Jr., Regulation of mTOR function in response to hypoxia by REDD1 and the TSC1/TSC2 tumor suppressor complex. *Genes Dev.* **18**, 2893–2904 (2004).
29. H. Maruta, J. Holden, A. Sizeland, G. D'Abaco, The residues of Ras and Rap proteins that determine their GAP specificities. *J. Biol. Chem.* **266**, 11661–11668 (1991).
30. K. Scheffzek, M. R. Ahmadian, W. Kabsch, L. Wiesmuller, A. Lautwein, F. Schmitz, A. Wittinghofer, The Ras-RasGAP complex: Structural basis for GTPase activation and its loss in oncogenic Ras mutants. *Science* **277**, 333–338 (1997).
31. M. Barbacid, *ras* genes. *Annu. Rev. Biochem.* **56**, 779–827 (1987).
32. U. Krengel, I. Schlichting, A. Scherer, R. Schumann, M. Frech, J. John, W. Kabsch, E. F. Pai, A. Wittinghofer, Three-dimensional structures of H-*ras* p21 mutants: Molecular basis for their inability to function as signal switch molecules. *Cell* **62**, 539–548 (1990).
33. C. Calés, J. F. Hancock, C. J. Marshall, A. Hall, The cytoplasmic protein GAP is implicated as the target for regulation by the *ras* gene product. *Nature* **332**, 548–551 (1988).
34. E. Im, F. C. von Lintig, J. Chen, S. Zhuang, W. Qui, S. Chowdhury, P. F. Worley, G. R. Boss, R. B. Pilz, Rheb is in a high activation state and inhibits B-Raf kinase in mammalian cells. *Oncogene* **21**, 6356–6365 (2002).
35. Y. Li, K. Inoki, K. L. Guan, Biochemical and functional characterizations of small GTPase Rheb and TSC2 GAP activity. *Mol. Cell. Biol.* **24**, 7965–7975 (2004).
36. M. Sattler, J. Schleucher, C. Griesinger, Heteronuclear multidimensional NMR experiments for the structure determination of proteins in solution employing pulsed field gradients. *Prog. Nucl. Magn. Reson. Spectrosc.* **34**, 93–158 (1999).
37. Y. Ito, K. Yamasaki, J. Iwahara, T. Terada, A. Kamiya, M. Shirouzu, Y. Muto, G. Kawai, S. Yokoyama, E. D. Laue, M. Walchli, T. Shibata, S. Nishimura, T. Miyazawa, Regional polysterism in the GTP-bound form of the human c-Ha-Ras protein. *Biochemistry* **36**, 9109–9119 (1997).
38. D. S. Wishart, B. D. Sykes, F. M. Richards, The chemical shift index: A fast and simple method for the assignment of protein secondary structure through NMR spectroscopy. *Biochemistry* **31**, 1647–1651 (1992).
39. J. John, R. Sohmen, J. Feuerstein, R. Linke, A. Wittinghofer, R. S. Goody, Kinetics of interaction of nucleotides with nucleotide-free H-*ras* p21. *Biochemistry* **29**, 6058–6065 (1990).
40. P. H. Seeburg, W. W. Colby, D. J. Capon, D. V. Goeddel, A. D. Levinson, Biological properties of human c-Ha-*ras*1 genes mutated at codon 12. *Nature* **312**, 71–75 (1984).
41. P. Gideon, J. John, M. Frech, A. Lautwein, R. Clark, J. E. Scheffler, A. Wittinghofer, Mutational and kinetic analyses of the GTPase-activating protein (GAP)-p21 interaction: The C-terminal domain of GAP is not sufficient for full activity. *Mol. Cell. Biol.* **12**, 2050–2056 (1992).
42. M. R. Ahmadian, T. Zor, D. Vogt, W. Kabsch, Z. Selinger, A. Wittinghofer, K. Scheffzek, Guanosine triphosphatase stimulation of oncogenic Ras mutants. *Proc. Natl. Acad. Sci. U.S.A.* **96**, 7065–7070 (1999).
43. J. John, M. Frech, A. Wittinghofer, Biochemical properties of Ha-ras encoded p21 mutants and mechanism of the autophosphorylation reaction. *J. Biol. Chem.* **263**, 11792–11799 (1988).
44. C. Kötting, K. Gerwert, Time-resolved FTIR studies provide activation free energy, activation enthalpy and activation entropy for GTPase reactions. *Chem. Phys.* **307**, 227–232 (2004).

45. K. Rittinger, P. A. Walker, J. F. Eccleston, S. J. Smerdon, S. J. Gamblin, Structure at 1.65 Å of RhoA and its GTPase-activating protein in complex with a transition-state analogue. *Nature* **389**, 758–762 (1997).
46. O. Daumke, M. Weyand, P. P. Chakrabarti, I. R. Vetter, A. Wittinghofer, The GTPase-activating protein Rap1GAP uses a catalytic asparagine. *Nature* **429**, 197–201 (2004).
47. A. C. Jones, M. M. Shyamsundar, M. W. Thomas, J. Maynard, S. Idziaszczyk, S. Tomkins, J. R. Sampson, J. P. Cheadle, Comprehensive mutation analysis of TSC1 and TSC2-and phenotypic correlations in 150 families with tuberous sclerosis. *Am. J. Hum. Genet.* **64**, 1305–1315 (1999).
48. M. M. Maheshwar, J. P. Cheadle, A. C. Jones, J. Myring, A. E. Fryer, P. C. Harris, J. R. Sampson, The GAP-related domain of tuberin, the product of the TSC2 gene, is a target for missense mutations in tuberous sclerosis. *Hum. Mol. Genet.* **6**, 1991–1996 (1997).
49. S. L. Dabora, S. Jozwiak, D. N. Franz, P. S. Roberts, A. Nieto, J. Chung, Y. S. Choy, M. P. Reeve, E. Thiele, J. C. Egelhoff, J. Kasprzyk-Obara, D. Domanska-Pakiela, D. J. Kwiatkowski, Mutational analysis in a cohort of 224 tuberous sclerosis patients indicates increased severity of TSC2, compared with TSC1, disease in multiple organs. *Am. J. Hum. Genet.* **68**, 64–80 (2001).
50. K. S. Au, J. A. Rodriguez, J. L. Finch, K. A. Volcik, E. S. Roach, M. R. Delgado, E. Rodriguez Jr., H. Northrup, Germ-line mutational analysis of the TSC2 gene in 90 tuberous-sclerosis patients. *Am. J. Hum. Genet.* **62**, 286–294 (1998).
51. K. S. Au, A. T. Williams, E. S. Roach, L. Batchelor, S. P. Sparagana, M. R. Delgado, J. W. Wheless, J. E. Baumgartner, B. B. Roa, C. M. Wilson, T. K. Smith-Knuppel, M. Y. Cheung, V. H. Whittemore, T. M. King, H. Northrup, Genotype/phenotype correlation in 325 individuals referred for a diagnosis of tuberous sclerosis complex in the United States. *Genet. Med.* **9**, 88–100 (2007).
52. N. Langkau, N. Martin, R. Brandt, K. Zugge, S. Quast, G. Wiegele, A. Jauch, M. Rehm, A. Kuhl, M. Mack-Vetter, L. B. Zimmerhackl, B. Janssen, TSC1 and TSC2 mutations in tuberous sclerosis, the associated phenotypes and a model to explain observed TSC1/TSC2 frequency ratios. *Eur. J. Pediatr.* **161**, 393–402 (2002).
53. N. D. Rendtorff, B. Bjerregaard, M. Frodin, S. Kjaergaard, H. Hove, F. Skovby, K. Brondum-Nielsen, M. Schwartz, Analysis of 65 tuberous sclerosis complex (TSC) patients by TSC2 DGGE, TSC1/TSC2 MLPA, and TSC1 long-range PCR sequencing, and report of 28 novel mutations. *Hum. Mutat.* **26**, 374–383 (2005).
54. R. L. Beauchamp, A. Banwell, P. McNamara, M. Jacobsen, E. Higgins, H. Northrup, P. Short, K. Sims, L. Ozelius, V. Ramesh, Exon scanning of the entire TSC2 gene for germline mutations in 40 unrelated patients with tuberous sclerosis. *Hum. Mutat.* **12**, 408–416 (1998).
55. A. Scrima, C. Thomas, D. Deaconescu, A. Wittinghofer, The Rap-RapGAP complex: GTP hydrolysis without catalytic glutamine and arginine residues. *EMBO J.* **27**, 1145–1153 (2008).
56. A. Eberth, R. Dvorsky, C. F. Becker, A. Beste, R. S. Goody, M. R. Ahmadian, Monitoring the real-time kinetics of the hydrolysis reaction of guanine nucleotide–binding proteins. *Biol. Chem.* **386**, 1105–1114 (2005).
57. J. John, I. Schlichting, E. Schiltz, P. Rosch, A. Wittinghofer, C-terminal truncation of p21H preserves crucial kinetic and structural properties. *J. Biol. Chem.* **264**, 13086–13092 (1989).
58. A. Shutes, C. J. Der, Real-time in vitro measurement of intrinsic and Ras GAP-mediated GTP hydrolysis. *Methods Enzymol.* **407**, 9–22 (2006).
59. A. Löw, M. Sprinzl, S. Limmer, Nucleotide binding and GTP hydrolysis by the 21-kDa product of the c-H-*ras* gene as monitored by proton-NMR spectroscopy. *Eur. J. Biochem.* **213**, 781–788 (1993).
60. Y. Li, K. Inoki, H. Vikis, K. L. Guan, Measurements of TSC2 GAP activity toward Rheb. *Methods Enzymol.* **407**, 46–54 (2006).
61. A. R. Tee, B. D. Manning, P. P. Roux, L. C. Cantley, J. Blenis, Tuberous sclerosis complex gene products, Tuberin and Hamartin, control mTOR signaling by acting as a GTPase-activating protein complex toward Rheb. *Curr. Biol.* **13**, 1259–1268 (2003).
62. K. Scheffzek, M. R. Ahmadian, GTPase activating proteins: Structural and functional insights 18 years after discovery. *Cell. Mol. Life Sci.* **62**, 3014–3038 (2005).
63. P. P. Chakrabarti, O. Daumke, Y. Suveyzdis, C. Kotting, K. Gerwert, A. Wittinghofer, Insight into catalysis of a unique GTPase reaction by a combined biochemical and FTIR approach. *J. Mol. Biol.* **367**, 983–995 (2007).
64. C. Kötting, A. Kallenbach, Y. Suveyzdis, A. Wittinghofer, K. Gerwert, The GAP arginine finger movement into the catalytic site of Ras increases the activation entropy. *Proc. Natl. Acad. Sci. U.S.A.* **105**, 6260–6265 (2008).
65. A. Warshel, P. K. Sharma, M. Kato, Y. Xiang, H. Liu, M. H. Olsson, Electrostatic basis for enzyme catalysis. *Chem. Rev.* **106**, 3210–3235 (2006).
66. T. Brinkmann, O. Daumke, U. Herbrand, D. Kuhlmann, P. Stege, M. R. Ahmadian, A. Wittinghofer, Rap-specific GTPase activating protein follows an alternative mechanism. *J. Biol. Chem.* **277**, 12525–12531 (2002).
67. P. Schanda, V. Forge, B. Brutscher, Protein folding and unfolding studied at atomic resolution by fast two-dimensional NMR spectroscopy. *Proc. Natl. Acad. Sci. U.S.A.* **104**, 11257–11262 (2007).
68. I. Schlichting, G. Rapp, J. John, A. Wittinghofer, E. F. Pai, R. S. Goody, Biochemical and crystallographic characterization of a complex of c-Ha-*ras* p21 and caged GTP with flash photolysis. *Proc. Natl. Acad. Sci. U.S.A.* **86**, 7687–7690 (1989).
69. F. Delaglio, S. Grzesiek, G. W. Vuister, G. Zhu, J. Pfeifer, A. Bax, NMRPipe: A multidimensional spectral processing system based on UNIX pipes. *J. Biomol. NMR* **6**, 277–293 (1995).
70. T. Schwede, J. Kopp, N. Guex, M. C. Peitsch, SWISS-MODEL: An automated protein homology-modeling server. *Nucleic Acids Res.* **31**, 3381–3385 (2003).

71. This work was supported by a grant from the Cancer Research Society (Canada) and a U.S. Department of Defense Tuberous Sclerosis Complex Research Program Award to V.S. A grant from the Canada Foundation for Innovation funded the 800-MHz NMR spectrometer. C.B.M. was supported by a postdoctoral fellowship from the Canadian Institutes of Health Research. M.I. and V.S. hold Canada Research Chairs and V.S. holds an Early Researcher Award from the Government of Ontario. We thank D. Moskau (Bruker Biospin AG, Fällanden, Switzerland) for data collection with a 1.7-mm cryoprobe and M. Yang, K. Su, and C. Fisher for assistance in the laboratory.

Submitted 8 September 2008
Accepted 24 December 2008
Final Publication 27 January 2009
10.1126/scisignal.2000029
Citation: C. B. Marshall, J. Ho, C. Buerger, M. J. Plevin, G.-Y. Li, Z. Li, M. Ikura, V. Stambolic, Characterization of the intrinsic and TSC2-GAP–regulated GTPase activity of Rheb by real-time NMR. *Sci. Signal.* **2**, ra3 (2009).